Journal of Photochemistry and Photobiology A: Chemistry 218 (2011) 93–100

Contents lists available at ScienceDirect

Journal of Photochemistry and Photobiology A: Chemistry

journal homepage: www.elsevier.com/locate/jphotochem

# A photolysis study on superoxide quenching at water/oil interface of Aerosol OT reversed micelle

Keishi Ohara*, Akihiro Ikeda, Shin-ichi Nagaoka

*Department of Chemistry, Graduate School of Science and Engineering, Ehime University, Matsuyama 790-8577, Japan*

ARTICLE INFO

*Article history:*
Received 1 September 2010
Received in revised form
10 November 2010
Accepted 8 December 2010
Available online 16 December 2010

*Keywords:*
Superoxide
Antioxidant
Vitamin C
Vitamin E
Photolysis
Reversed micelle
Tocopherol

ABSTRACT

The quenching kinetics of superoxide ($O_2^{-\bullet}$) in water/oil (w/o) interface region of Aerosol OT reversed micelle has been investigated with a transient absorption method. Photodecomposition of α-tocopherol by 266 nm laser light in the presence of $O_2$ produced $O_2^{-\bullet}$ together with the tocopheroxyl radical (Toc•). The subsequent reaction between Toc• and $O_2^{-\bullet}$ occurred in the time region of 1–150 μs after the photoexcitation. There, $O_2^{-\bullet}$ kinetics could be traced by monitoring the Toc• absorption. In an Aerosol OT reversed micelle solution containing vitamin C (VC), VC would be located in water droplets inside the reversed micelle and would react with both Toc• and $O_2^{-\bullet}$ at the w/o interface around the reversed micelle. The Toc• decay in the time region of 1–150 μs was accelerated by addition of VC, suggesting that the $O_2^{-\bullet}$ quenching by VC progressed as well as the Toc• quenching by VC. From a numerical simulation with treating the simultaneous rate equations for Toc• concentration by Runge–Kutta method, the rate constant for the $O_2^{-\bullet}$ quenching by VC could be estimated to be $6.9 \times 10^7\ M^{-1}\ s^{-1}$. This value is much larger than the corresponding value reported in homogeneous water solution, suggesting that the $O_2^{-\bullet}$ quenching by VC indeed occurred at the w/o interface of the reversed micelle.



## 1. Introduction

Oxidative stresses to living things can cause injuries and diseases. Reactive oxygen species (ROS), such as the hydroxyl radical (HO•), the superoxide anion radical ($O_2^{-\bullet}$), and singlet oxygen ($^1O_2$), are indeed generated through biological processes, and are thought to act vital roles in living things [1–3]. Antioxidants opposing oxidative stresses are contained in biological systems and are believed to work against ROS [3–9]. Many natural antioxidants, such as vitamin E (VE), vitamin C (VC), and plant-origin polyphenols, are widely distributed, so animals and human being can ingest them from daily meals [10,11]. Activities and working mechanism of such substances against ROS and other active species have been subjects of numerous studies in pharmacological, medical, agricultural, food-science, and also industrial divisions. In these situations, many antioxidant assays have been developed and applied [11–15].

$O_2^{-\bullet}$ that is the one-electron reductant form of molecular oxygen ($O_2$) is generated through aerobic metabolisms in biological systems [16]. Besides, $O_2^{-\bullet}$ is a precursor of some ROS such as the hydroperoxyl radical (HOO•), HO•, hydrogen peroxide ($H_2O_2$), and $^1O_2$ [17,18]. Although $O_2^{-\bullet}$ might cause degradation and diseases in biological systems [19], those are thought to be limited because $O_2^{-\bullet}$ is usually quenched rapidly there by superoxide dismutase (SOD) through dismutation. In laboratory research, some methods can be applied for generating $O_2^{-\bullet}$, for example, $O_2^{-\bullet}$ generation from potassium superoxide ($KO_2$) or that from xanthine oxidase and xanthine system. $O_2^{-\bullet}$ is quenched by some antioxidants such as VC or plant-origin phenol derivatives [20,21], and also by free radicals such as the tocopheroxyl radical (Toc•), the ascorbate monoanion radical ($As^{-\bullet}$), and nitric oxide (NO•). The $O_2^{-\bullet}$ scavenging by natural antioxidants has been an attractive theme as well as scavenging of the other ROS. The antioxidant capacities of many substances against $O_2^{-\bullet}$ have been measured with some methods such as SOD activation assay, chemi-luminescence assay, and spin-trapping EPR assay [13,20–27]. These methods, which are based on competition kinetics, have given useful parameters for the $O_2^{-\bullet}$ scavenging capacity and numerous data have been stocked. However, most of the methods have given no absolute rate constant for the $O_2^{-\bullet}$ scavenging reactions. On the other hand, in pulse-radiolysis, $O_2^{-\bullet}$ is generated by the reaction between solvated electron ($e^-_{solv}$) and $O_2$ or by other reactions, and the rate constants for the $O_2^{-\bullet}$ scavenging have been determined by time-resolved measurements [28,29]. The pulse-radiolysis experiments can give a reliable rate constant for the $O_2^{-\bullet}$ quenching, but those are complicated instrumentally. Another time-resolved method for estimating the $O_2^{-\bullet}$ quenching rate constant is needed especially when investigating $O_2^{-\bullet}$ kinetics in inhomogeneous media such as micelles and membranes.

Previously, we investigated photogeneration and decay kinetics of Toc• in a homogeneous solution and an emulsion system

* Corresponding author. Tel.: +81 89 927 9596; fax: +81 89 927 9590.
*E-mail address:* ohara@chem.sci.ehime-u.ac.jp (K. Ohara).

1010-6030/$ – see front matter © 2010 Elsevier B.V. All rights reserved.
doi:10.1016/j.jphotochem.2010.12.008

by a transient absorption method [30]. As well-known, tocopherol (TocH) is decomposed by ultraviolet (UV) light (UV-B, <310 nm) [30–32]. This decomposition produces Toc• and $e^-_{solv}$ through an electron-ejection in the excited state TocH ($^1TocH^*$) and the subsequent proton ($H^+$) releasing (reaction (1)) [30–32]. Under deoxygenated or low $O_2$ concentration conditions, some of Toc• and $e^-_{solv}$ recombine within a few microseconds, and reproduce TocH (reaction (2)). The remaining Toc• usually decays slowly in a few seconds or more through a bimolecular self-quenching process (reaction (3)). In addition to these processes, in the presence of oxygen, $e^-_{solv}$ is quenched rapidly by $O_2$ and produces $O_2^{-\bullet}$ (reaction (4)). Subsequently, $O_2^{-\bullet}$ reacts rapidly with Toc• and reproduces TocH (reaction (5)) [30,31].

$$TocH + h\nu \rightarrow {}^1TocH^* \rightarrow Toc^\bullet + e^-_{solv} + H^+ \quad (1)$$

$$Toc^\bullet + e^-_{solv} + H^+ \rightarrow TocH \quad (2)$$

$$Toc^\bullet + Toc^\bullet \rightarrow \text{products} \quad (3)$$

$$e^-_{solv} + O_2 \rightarrow O_2^{-\bullet} \quad (4)$$

$$Toc^\bullet + O_2^{-\bullet} + H^+ \rightarrow TocH + O_2 \quad (5)$$

$O_2^{-\bullet}$ might also be quenched by TocH, but its contribution in the total $O_2^{-\bullet}$ quenching is negligible because the rate constant of this process is small ($<2 \times 10^4\ M^{-1}\ s^{-1}$). These facts suggest that the $O_2^{-\bullet}$ dynamics can be monitored by the transient absorption of Toc• in homogeneous solutions and even in inhomogeneous systems such as micelle solutions and emulsions. When another antioxidant such as VC coexists in the system, the Toc• decay would be sensitively affected through the $O_2^{-\bullet}$ quenching by the antioxidant (reaction (7)) as well as through the Toc• reduction by the antioxidant (reaction (6)). In this way, the rate constant for the $O_2^{-\bullet}$ quenching by the antioxidant might be estimated from the Toc• decay data.

$$Toc^\bullet + VC \rightarrow TocH + VC^\bullet \quad (6)$$

$$O_2^{-\bullet} + VC \rightarrow \text{products} \quad (7)$$

In this paper, in order to investigate the $O_2^{-\bullet}$ quenching kinetics at water/oil (w/o) interface, a laser photolysis study for $\alpha$-tocopherol ($\alpha$-TocH) has been performed in Aerosol OT (AOT) reversed micelle solutions in the presence of $O_2$. In water-in-oil type dispersion such as the AOT reversed micelle, lipophilic TocH should be located in the bulk oil phase and a water-soluble antioxidant such as VC is in water droplets. Thus, the quenching reactions by VC for Toc• and $O_2^{-\bullet}$ generated by the photolysis of TocH should progress mainly at the w/o interface of the reversed micelle. The time-dependent transient absorption data obtained for Toc• in 1–150 μs time region were analyzed based on simultaneous differential rate equations for Toc• using 4th-order Runge–Kutta (RK4) method. The RK4 method is a widely-used numerical integration way to solve simultaneous differential equations [33–35]. From the analysis, the rate constant for the antioxidant reaction of VC against $O_2^{-\bullet}$ occurring at the w/o interface of the AOT reversed micelle has been determined.

## 2. Experimental

$\alpha$-Tocopherol and ascorbic acid (VC) were obtained from Wako Pure Chemicals, and were used as received. Aerosol OT (sodium bis(2-ethyl-1-hexyl)sulfosuccinate) was a commercially available reagent (TCI) and was used as received. Isooctane (2,2,4-trimethylpentane) from Wako was used as received. Deionized water was treated by an ion-exchange column (Millipore Milli-Q). The concentration of AOT in isooctane was kept at $1.0 \times 10^{-1}$ mol dm$^{-3}$ (M). The ratio of water and isooctane (w/o value) in sample solutions was kept at 1/100 (v/v) [36]

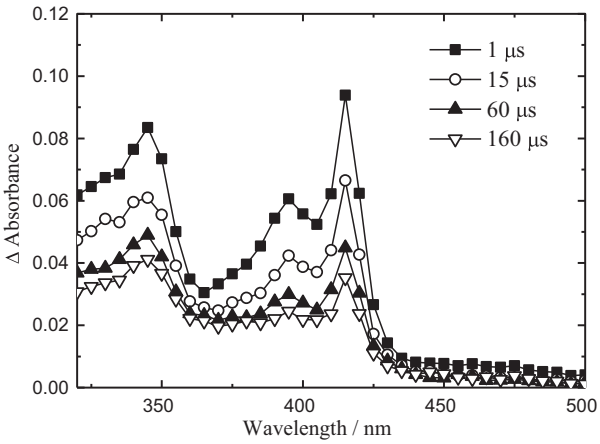


**Fig. 1.** Time evolution of the transient absorption spectrum in the photolysis of $\alpha$-TocH ($4.00 \times 10^{-4}$ M) in an AOT reversed micelle solution.

Procedure of transient absorption experiments was the same as that reported previously [30,37]. Transient absorption spectra were measured at room temperature with a nanosecond laser-photolysis system (UNISOKU TSP-1000), using an Nd-YAG laser (Continuum Surelight-I, FHG 266 nm, FWHM < 5 ns, 2 Hz) as an excitation light source. Additional sharp-cut filters (UV30 or Y50) were used for cutting the laser scattering light and the second-order diffraction light. The probe light was set to pass through an 1-cm square quartz cell at 2 mm position from the cell side emitted by the excitation laser. Time profiles of the transient absorption were obtained by accumulating 4–16 waves with a digital oscilloscope (Sony-Tektronix TDS3032). For reducing oxygen dissolved in sample solutions, $N_2$ gas bubbled for 5 min before the experiment.

Steady-state EPR spectra were measured at room temperature with a JEOL FA-100 EPR spectrometer using 100 kHz field modulation (modulation width 0.05 mT). Sample solutions flowed through a quartz flat cell (optical path: 1 mm) and were irradiated in the EPR cavity by an Nd-YAG laser (Continuum Surelight-I, FHG 266 nm, 9.7 Hz) during the measurements.

Double-mixing stopped-flow measurements were carried out at 25 °C with a UNISOKU RSP-1000 stopped-flow system [38]. Toc• was prepared by mixing equal volumes of $\alpha$-TocH and the aryloxyl radical solutions 2 s prior to the mixing of equal volumes of VC and Toc• solutions using the double-mixing unit. Detailed procedure on experiments and analysis have already been reported [38].

## 3. Results and discussion

### 3.1. Photolysis of α-TocH in an AOT solution without another antioxidant

Fig. 1 shows time development of the transient absorption spectrum observed in photolysis of $\alpha$-TocH in an AOT reversed micelle solution. An absorption band at 320–440 nm, which appeared within 15 ns from the excitation laser pulse and decayed with time, is due to Toc• [30]. It indicates that the photodecomposition of $\alpha$-TocH occurred through reaction (1) in the AOT solution, as well as in ethanol. The absorption maxima of Toc• in the AOT system (415 nm and 395 nm) blue-shifted by ~10 nm from those reported for Toc• in ethanol [30], and the peak wavelengths agreed with those reported for Toc• in *n*-hexane and *n*-heptane [35]. This fact suggests that Toc• in this system is located in hydrophobic medium, probably in the bulk isooctane phase of the reversed micelle solution. On the other hand, the broad absorption band due to $e^-_{solv}$ at 540–700 nm was observed, but its intensity was very small compared with that reported in the homogeneous solutions [30,31].

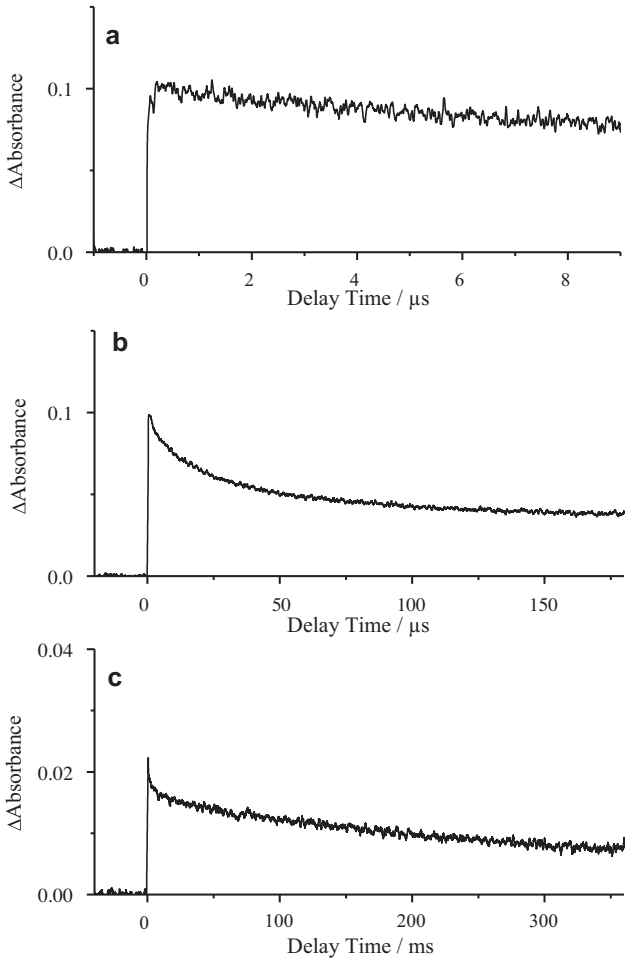


**Fig. 2.** Time profiles of the transient absorption at 415 nm in the photolysis of α-TocH ($4.00 \times 10^{-4}$ M) in an AOT reversed micelle solution. High-frequency random-noise was removed by a smoothing method.

Some rapid reactions might quench $e^-_{solv}$ produced by reaction (1).

Fig. 2 shows time profiles of the transient absorption at 415 nm observed in the photolysis of α-TocH in the AOT reversed micelle solution. The decay curve of Toc• consisted of two components having different time constants. One is a decay observed in the time region of 1–150 μs and another is a very slow decay component observed in the time region more than 10 ms. The slow component is thought to be due to the second-order decay coming from the bimolecular self-quenching of Toc• (reaction (3)), as well as that reported for a homogeneous ethanol solution [30]. The fast decay component in the range of 1–150 μs is thought to be due to the reaction between Toc• and $O_2^{-\bullet}$ (reaction (5)). There, $O_2^{-\bullet}$ had been produced by the rapid reaction between $e^-_{solv}$ and $O_2$ dissolving in the solution (reaction (4)). It was confirmed by the fact that contribution of this decay component decreased effectively by deoxygenating. In the photolysis in ethanol, the rapid decay, whose time constant was 0.64 μs, due to the recombination process between Toc• and $e^-_{solv}$ (reaction (2)) was observed in the transient absorption both at 425 nm (Toc•) and at 620 nm ($e^-_{solv}$) [30]. However, such a rapid decay component for Toc• was negligible in the present AOT reversed micelle system, while the weak absorption band due to $e^-_{solv}$ diminished with the time constant of 0.23 μs. This $e^-_{solv}$ lifetime is a little smaller or comparable to those reported [39–41]. The rapid quenching of $e^-_{solv}$ by AOT might progress in addition to reaction (4). Moreover, reaction (2) might be largely inhibited since lipophilic Toc• and hydrophilic $e^-_{solv}$ were separated from each other soon after their generation at the reversed micelle interface.

In this situation, the Toc• decay by reaction (5) can be treated with a second-order rate equation represented as the following Eq. (8) [30].

$$\frac{d[\text{Toc}^\bullet]}{dt} = -k_5[\text{Toc}^\bullet][O_2^{-\bullet}] \tag{8}$$

Here, $k_5$ is the second-order rate constant for reaction (5), and [Toc•] and [$O_2^{-\bullet}$] are the concentrations of Toc• and $O_2^{-\bullet}$, respectively. In this time region, the same amounts of Toc• and $O_2^{-\bullet}$ are decreased only by reaction (5), and the initial concentration of $O_2^{-\bullet}$ ($[O_2^{-\bullet}]_0$) should be smaller than that of Toc• ($[\text{Toc}^\bullet]_0$) because $e^-_{solv}$ producing $O_2^{-\bullet}$ may be quenched by the other processes than reactions (2) and (4). Then, assuming that $\Delta = [\text{Toc}^\bullet] - [O_2^{-\bullet}]$ is constant ($\Delta > 0$), the time-development of [Toc•] can be represented by the following Eq. (9).

$$[\text{Toc}\bullet] = \frac{\Delta}{1 - f\ \exp(-\Delta k_5 t)} \tag{9}$$

Here, $f = [O_2^{-\bullet}]_0/[\text{Toc}^\bullet]_0$. Using $\varepsilon = 3.08 \times 10^3\ \text{M}^{-1}\ \text{cm}^{-1}$ (the value at 418 nm in *n*-heptane [35]) as the molar absorption coefficient of Toc• at 415 nm, we could estimate $k_5 = (1.32 \pm 0.045) \times 10^9\ \text{M}^{-1}\ \text{s}^{-1}$, $\Delta = 1.22 \times 10^{-5}$ M and $f = 0.594$ from a least-squares fit of the time-profile data to Eq. (9). This $k_5$ value is a little smaller than the reported value ($2.19 \times 10^9\ \text{M}^{-1}\ \text{s}^{-1}$) in ethanol [30], and is one-order smaller than the diffusion-controlled limit in isooctane ($2.1 \times 10^{10}\ \text{M}^{-1}\ \text{s}^{-1}$ at 25 °C [42]), although the $k_5$ value is expected to be close to the diffusion control limit [31]. The viscosity of the AOT solutions might be larger than that of isooctane. Otherwise, the result might suggest that the diffusion of Toc• and/or $O_2^{-\bullet}$ was partially restricted by some reasons, for example, either Toc• or $O_2^{-\bullet}$ was partially trapped around the water droplets of the reversed micelle. It would be possible that the polar species such as $O_2^{-\bullet}$ were located near or in the water droplets. Such effect might decrease the apparent rate of the reaction between Toc• and $O_2^{-\bullet}$.

### 3.2. Photolysis of α-TocH in an AOT reversed micelle solution containing VC

Water-soluble antioxidants contained in reversed micelle solutions should be dissolved in water phase inside the reversed micelle. When free-radicals such as Toc• and $O_2^{-\bullet}$ are generated in the bulk oil phase, the water-soluble antioxidants would scavenge them in the w/o interface region around the reversed micelle. Fig. 3a shows time development of the transient absorption spectrum observed in photolysis of α-TocH in an AOT reversed micelle solution containing VC. The spectra are very similar to those in Fig. 1, suggesting that they consist of the absorption band due to Toc• generated by the photolysis of α-TocH. In addition, a small absorption band due to $As^{-\bullet}$ was observed around 370 nm (Fig. 3a) [43]. The reaction of Toc• with VC is thought to produce $As^{-\bullet}$ as a secondary product (reaction (6)). In this system, the water phase inside the reversed micelle should be acidic (pH 3–4) because of dissolved VC. In acidic solutions whose pH is less than 4, most of VC should exist as the non-dissociation form. Thus, in this system, the reaction of Toc• with the non-dissociation form of VC should occur, and the neutral radical of ascorbic acid ($AsH^\bullet$) should be generated in that instant through the hydrogen atom transfer reaction. The $pK_a$ value for the deprotonation of $AsH^\bullet$ is known to be −0.45 [44]. Then $As^{-\bullet}$ should be immediately produced from $AsH^\bullet$ by deprotonation, even in solutions whose pH was down to 0. In a previous TR-EPR study on the photoreaction in the aqueous micelle solutions at pH 2–11, the $As^{-\bullet}$ spectrum could be observed at the delay time within 0.5 μs after the photoexcitation even in acidic

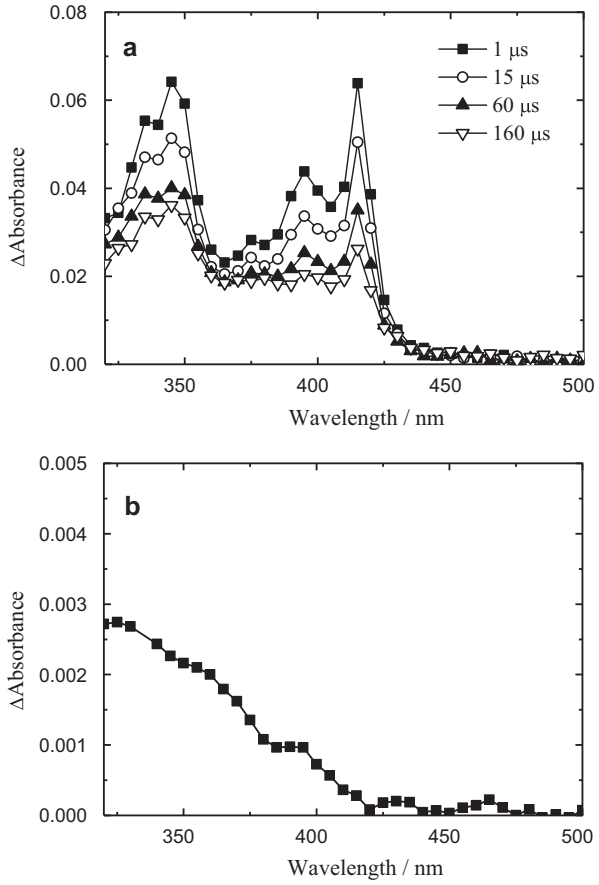


**Fig. 3.** (a) Time evolution of the transient absorption spectrum in the photolysis of $\alpha$-TocH ($4.00 \times 10^{-4}$ M) with VC ($1.00 \times 10^{-4}$ M) in an AOT reversed micelle solution. (b) Transient absorption spectrum observed in the photolysis of VC ($1.00 \times 10^{-4}$ M) in an AOT reversed micelle solution.

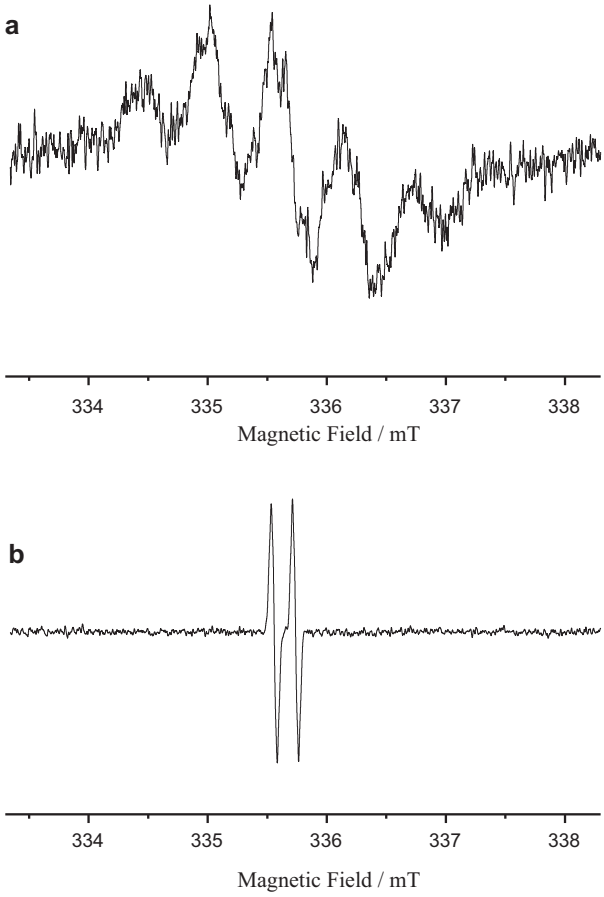


**Fig. 4.** Steady-state EPR spectra observed with irradiating 9.7 Hz laser (266 nm) to an AOT reversed micelle solution containing $\alpha$-TocH ($4.00 \times 10^{-4}$ M) without (a) and with (b) VC ($1.00 \times 10^{-4}$ M). Signal gain of (a) was ×10 of that of (b).

solutions [45]. Thus the deprotonation of AsH$^{\bullet}$ is thought to occur rapidly.

On the other hand, the photolysis of VC itself might occur since VC has absorption at 266 nm ($\varepsilon = 9.4 \times 10^3$ M$^{-1}$ cm$^{-1}$ in water). Fig. 4b shows the transient absorption spectrum obtained by irradiating an AOT reversed micelle solution containing VC without $\alpha$-TocH. Small absorption was observed at 320–410 nm and it did not decay with time. Thus, this band is thought to be due to As$^{-\bullet}$ and some photoreaction products. The efficiency of the photodecomposition of VC is thought to be much smaller than that of $\alpha$-TocH.

Fig. 4 shows steady-state EPR spectra observed with irradiating 9.7 Hz laser (266 nm) to an AOT reversed micelle solution containing $\alpha$-TocH with and without VC. In the absence of VC (Fig. 4a), the EPR spectrum spread over 5 mT width due to Toc$^{\bullet}$ ($g = 2.0046$) was obtained [30]. The Toc$^{\bullet}$ EPR signals immediately vanished when stopping laser irradiation. The result indicates that Toc$^{\bullet}$ was produced by photolysis and decayed within a few seconds. The Toc$^{\bullet}$ spectrum obtained in the AOT solution was rather broadened from that obtained in a homogeneous ethanol solution of $\alpha$-TocH [30]. This line-broadening might come from the fast spin-spin relaxation in Toc$^{\bullet}$, suggesting that Toc$^{\bullet}$ was located in the w/o interface region near the micelle and its motion was partially restricted.

On the other hand, in the EPR spectrum observed with irradiating 9.7 Hz laser to an AOT reversed micelle solution containing $\alpha$-TocH and VC (Fig. 4b), a couple of hyperfine lines ($A_H = 0.18$ mT) due to As$^{-\bullet}$ were observed at $g = 2.0050$ [36,44]. No EPR line due to the other species including Toc$^{\bullet}$ was observed there. The result indicates that photogenerated Toc$^{\bullet}$ was immediately reduced by VC and As$^{-\bullet}$ was produced with TocH (reaction (6)). In this system, the photolysis of VC itself might occur simultaneously. In fact, in the EPR spectrum measured for an AOT solution containing only VC (without $\alpha$-TocH), the EPR lines due to As$^{-\bullet}$ were also observed. However, their intensities were less than 1/5 of those observed for the solution containing both $\alpha$-TocH and VC (Fig. 4b). As generally known, the lifetime of As$^{-\bullet}$ is much larger than that of Toc$^{\bullet}$ in solutions. Taking account of this fact, we consider that the photolysis efficiency of VC is much smaller than that of $\alpha$-TocH and As$^{-\bullet}$ generated by the photolysis of VC itself may not largely affect the Toc$^{\bullet}$ kinetics.

Fig. 5 shows time profiles of the transient absorption at 415 nm due to Toc$^{\bullet}$ measured in the photolysis of $\alpha$-TocH in the AOT solution containing VC. As a result of the absorption of $\alpha$-TocH and VC, the transmittance at 266 nm of the solution through the measurement area (2 mm path) irradiated by the excitation laser in the cell was c.a. 60%. The decay curve of Toc$^{\bullet}$ also consisted of two components; one is a fast decay observed in the time region of 1–150 μs and another is a slow decay component observed in the time region of 1–50 ms. From the comparison between Figs. 2c and 5c, it is seen that the Toc$^{\bullet}$ decay was accelerated by addition of VC. The result suggests that the antioxidant reaction of VC against Toc$^{\bullet}$ (reaction (6)) occurred in this system. The Toc$^{\bullet}$ kinetics in this system would be explained in terms of reactions (1)–(6). From the stopped-flow studies in several media, it is known that the reaction between Toc$^{\bullet}$ and As$^{-\bullet}$ is negligible in kinetic measurements for Toc$^{\bullet}$ within a few seconds because the rate constant is small ($<10^3$ M$^{-1}$ s$^{-1}$). In the literature, the rate constant for the reaction between Toc$^{\bullet}$ and ascorbate is $2.73 \times 10^6$ M$^{-1}$ s$^{-1}$ in an ethanol/$H_2O$ mixed solvent (5:1, v/v) and $2.1 \times 10^5$ M$^{-1}$ s$^{-1}$ in a Triton X-100 micelle aqueous

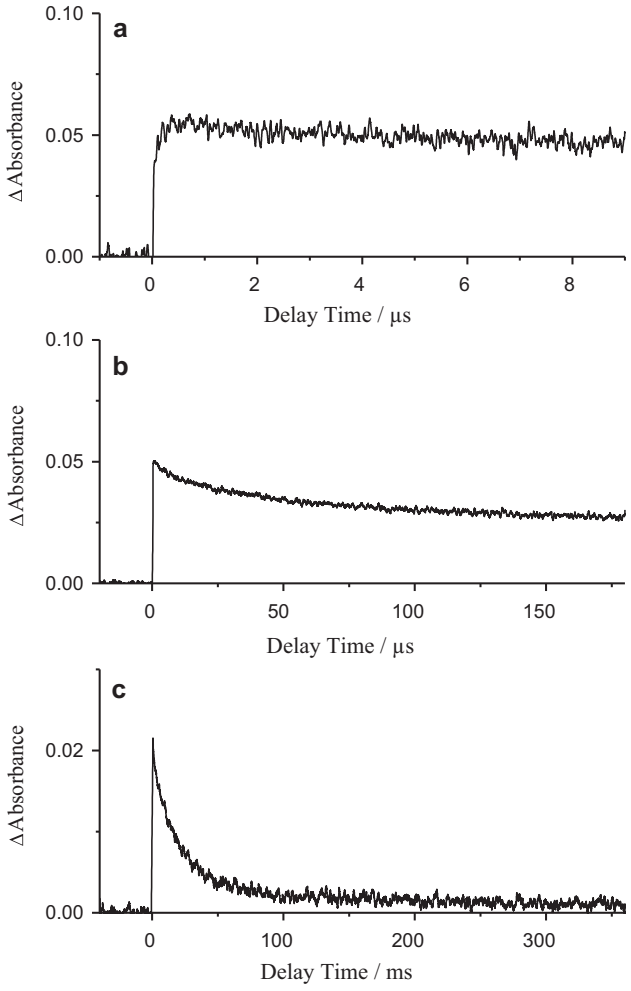


**Fig. 5.** Time profiles of the transient absorption at 415 nm in the photolysis of α-TocH ($4.00 \times 10^{-4}$ M) in an AOT reversed micelle solution containing VC ($1.00 \times 10^{-4}$ M).

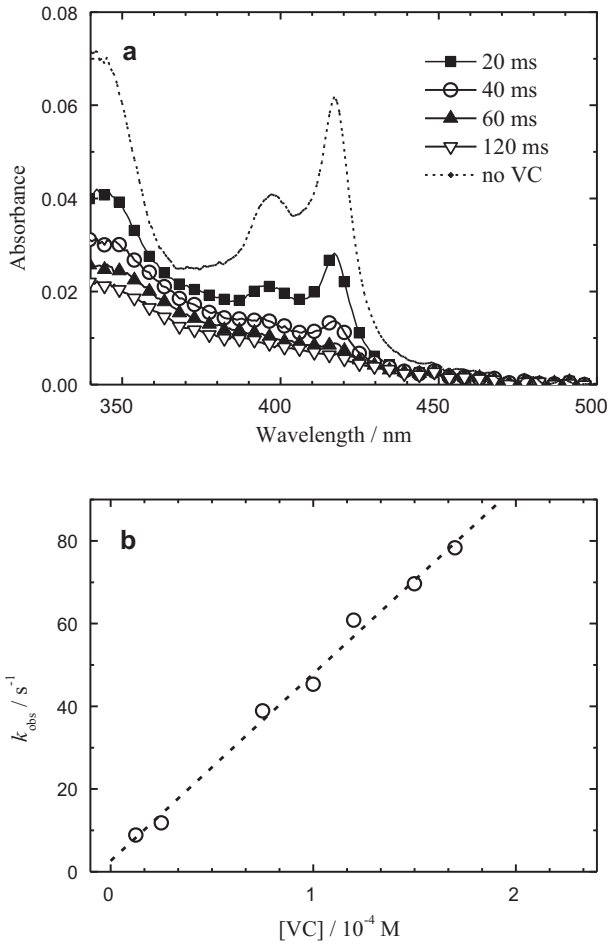


**Fig. 6.** (a) Time evolution of the absorption spectrum measured by the stopped-flow method after mixing an AOT solution containing Toc• and that containing VC ($1.00 \times 10^{-4}$ M). Broken line shows the Toc• spectrum observed after mixing solutions without containing VC. (b) Plots for $k_{obs}$ vs. [VC] for the reaction between Toc• and VC in an AOT reversed micelle solution.

solution [32,43]. Since the rate constant for the reaction between VC and Toc• was reported to be $10^4$–$10^6$ M$^{-1}$ s$^{-1}$ in several media, the acceleration due to VC should be observed only in the time region larger than milliseconds. In fact, the decay in the range of 1–100 ms (Fig. 5c) was largely accelerated by VC. There, the time constant of the Toc• decay was 21.9 ms. From this value, the second-order rate constant for the reaction between VC and Toc• was roughly estimated to be $4.6 \times 10^5$ M$^{-1}$ s$^{-1}$. This value is consistent with the reported rate constants. On the other hand, the second-order decay rate constant ($k_5$) estimated from the Toc• decay in the time region of 1–150 μs (Fig. 5b) was also somewhat increased by addition of VC.

We measured the second-order rate constant for the reaction between Toc• and VC in an AOT reversed micelle solution by using the double-mixing stopped-flow technique. There, by mixing equal volumes of the AOT solution containing Toc• and that containing VC, time decays of the Toc• absorption at 417 nm were measured for some [VC]s. Fig. 6a shows a typical time evolution of the absorption spectrum after mixing the Toc• solution and a solution containing VC. The broken line in Fig. 6a shows the Toc• spectrum obtained after mixing the Toc• solution and a control solution without VC. The Toc• spectrum in Fig. 6a resembles that obtained by the photolysis (Fig. 1) very much. The absorbance at 320–400 nm was relatively large compared with that in Fig. 1, suggesting the existence of some reaction products other than Toc•. The products may originate from the aryloxyl radical or others. From the absorbance at 417 nm obtained for the control solution (the broken line), the initial concentration of Toc• was estimated to be $2.0 \times 10^{-5}$ M and dead-time of the measurement by mixing was estimated to be 18 ms. After mixing the sample solution containing VC, the absorption band of Toc• around 417 nm decreased with time. The absorption band of $As^{-}$• generated by the reaction should be located around 370 nm, but was negligibly weak, probably because of its low concentration. The apparent decay rate constant ($k_{obs}$) of Toc• was determined by fitting each decay curve to a single exponential curve. From the slope of plots of $k_{obs}$ vs. [VC] shown in Fig. 6b, the second-order rate constant for the reaction between Toc• and VC was estimated to be $k_{6s} = (4.52 \pm 0.18) \times 10^5$ M$^{-1}$ s$^{-1}$. This value agreed with that estimated above from the transient absorption result and was comparable to that reported for a Triton X-100 micelle solution.

Although the rate constant for the reaction between Toc• and VC is no more than $4.5 \times 10^5$ M$^{-1}$ s$^{-1}$, the Toc• decay in the range of 1–150 μs was also accelerated by addition of VC. Fig. 7 shows a plot of $k_5$ value estimated apparently by fitting the decay data in the range of 1–150 μs to Eq. (9) vs. [VC]. The apparent $k_5$ value gradually increased with increase of [VC], not linearly but quadratically. If VC quenched only Toc•, the apparent $k_5$ value would increase linearly with increase of [VC]. The reason for the unexpected result should show that another reaction affecting the Toc• decay occurred in this time region. It would be $O_2^{-}$• quenching by VC, because the quenching should influence the Toc• kinetics through the reaction

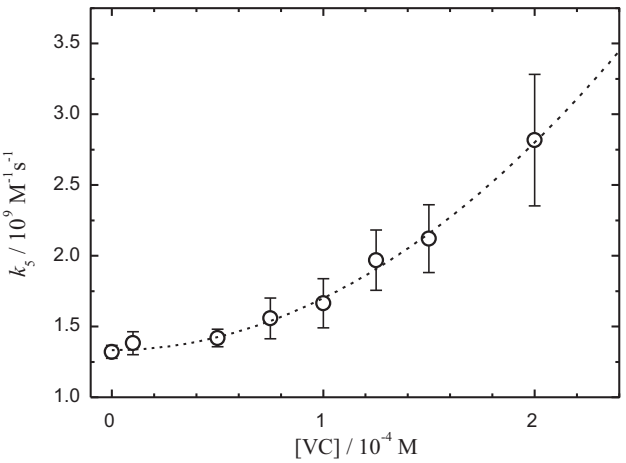


**Fig. 7.** Plot of the apparent $k_5$ value estimated by fitting the data to Eq. (9) vs. [VC].

between Toc• and $O_2^{-\bullet}$ (reaction (5)). Since the Toc• decay in the range of 1–150 μs, which would be mainly caused by reactions (5), was actually accelerated by addition of VC, the fast quenching of Toc• or $O_2^{-\bullet}$ occurred there. The rate constant for reaction (6) or (7) should be much larger than the $k_{6s}$ value estimated above.

This parabolic [VC] dependence of the $k_5$ value might be explained if VC quenches both Toc• and $O_2^{-\bullet}$. In this case, we have to treat this system with the following simultaneous differential rate equations.

$$\frac{d[\text{Toc}^\bullet]}{dt} = -k_5[\text{Toc}^\bullet][O_2^{-\bullet}] - k_6[\text{Toc}^\bullet][\text{VC}] \quad (10)$$

$$\frac{d[O_2^{-\bullet}]}{dt} = -k_5[\text{Toc}^\bullet][O_2^{-\bullet}] - k_7[O_2^{-\bullet}][\text{VC}] \quad (11)$$

Here, $k_6$ and $k_7$ are the second-order rate constants for reactions (6) and (7), respectively.

The other reactive species or minor products such as •OH and $H_2O_2$ might be in the system, and they might be possible to react to Toc•. •OH and $H_2O_2$ might be generated as secondary products in reactions of $O_2^{-\bullet}$. However, we think the effect of such species except for •OOH on the Toc• decay within 200 ms is negligible because the concentration of these species in samples should be very low in the laser photolysis measurements. If •OH was generated, it should react to TocH or VC whose concentration was much larger than that of Toc•. In order to explain the Toc• kinetics, we require the simultaneous reactions quenching both Toc• and $O_2^{-\bullet}$, such as reactions (6) and (7).

### 3.3. Estimation of the rate-constants by Runge–Kutta simulation

In order to estimate $k_6$ and $k_7$ values from the experimental results, we tried a numerical simulation of the simultaneous differential equations (Eqs. (10) and (11)) based on RK4 method using a spreadsheet application. In the simulation, the processes other than reactions (5), (6), and (7) were neglected. Here, $k_5$ value was set constant at the value ($1.32 \times 10^9$ $M^{-1}$ $s^{-1}$) obtained from the decay curve in the AOT solution without VC. A pseudo-first-order approximation was used for [VC] in reactions (6) and (7) for simplification of the simulation. In the measurements, [Toc•] was estimated to be always less than $3 \times 10^{-5}$ M from the peak absorbance (~0.10 at 415 nm). And the amount of Toc• related to the reactions (5), (6), and (7) was less than 60% of the total yield of Toc•. In this approximation, $k_6$[VC] and $k_7$[VC] values in Eqs. (10) and (11) were treated as time-independent parameters in the simulation. The $k_6$[VC] and $k_7$[VC] values were estimated for each [VC] from the best fitting result obtained by executing repeated RK4 calculation

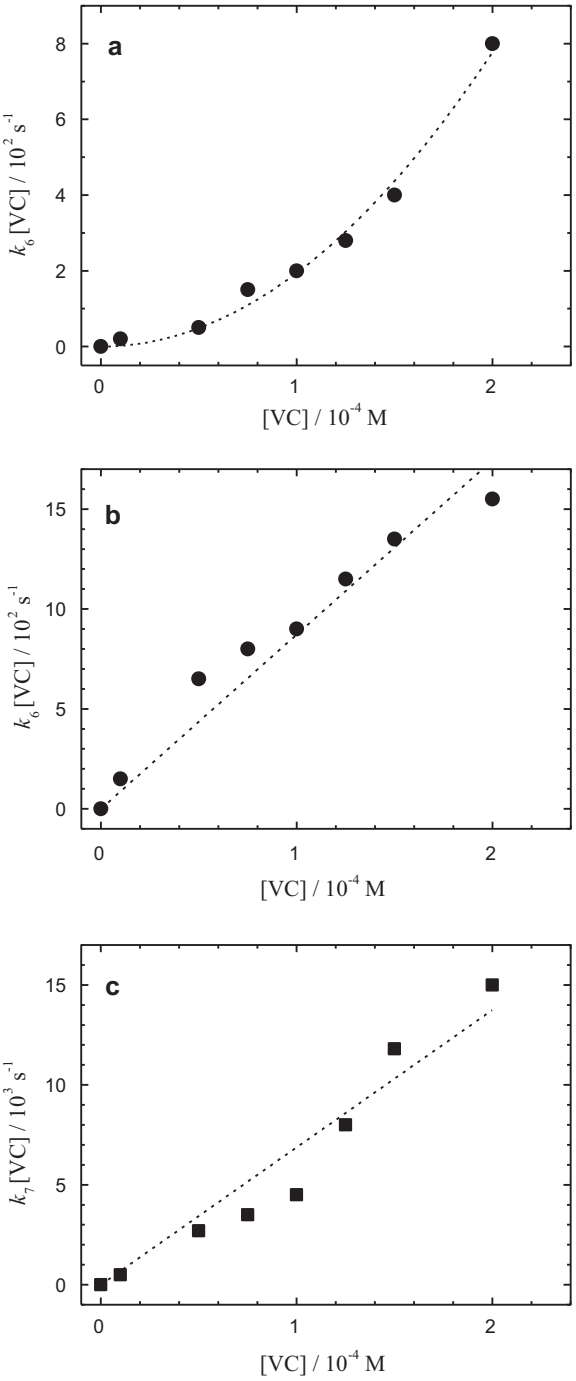


**Fig. 8.** (a) Plot of the $k_6$[VC] value (vs. [VC]) estimated by the RK4 simulation of Eqs. (10) and (11) on the assumption that $k_7 = 0$. Plots of the best results for (b) the $k_6$[VC] value and (c) the $k_7$[VC] value (vs. [VC]) estimated by the RK4 simulation of Eqs. (10) and (11), respectively.

so as to reproduce the Toc• time decay curve with varying the parameters.

First, for the model in which VC quenched only Toc•, an RK4 simulation was carried out on the assumption that reaction (7) was negligible ($k_7 = 0$). The $k_6$[VC] value estimated for each [VC] from the best fitting is plotted vs. [VC] in Fig. 8a. The plot shows a parabolic relation of $k_6$ [VC] with [VC]. Similar parabolic relation was obtained from the simulation for a plot of $k_7$[VC] vs. [VC] on the assumption that reaction (6) was negligible ($k_6 = 0$). These parabolic relations of the apparent rate constants ($k_6$[VC] and $k_7$[VC]) to [VC] are not reasonable because the second-order rate constant ($k_6$ or $k_7$) for

each reaction depends on [VC]. Then, both reactions (6) and (7) should participate in the Toc• decay kinetics in this system. The RK4 simulation varying both $k_6$ and $k_7$ was required.

Fig. 8b and c shows plots of $k_6$[VC] and $k_7$[VC] values (vs. [VC]) estimated from the best fit results of the RK4 simulation varying both $k_6$ and $k_7$. Linear relationship was obtained for each of $k_6$[VC] and $k_7$[VC]. The values $k_6 = (8.7 \pm 0.4) \times 10^6\ M^{-1}\ s^{-1}$ and $k_7 = (6.9 \pm 0.4) \times 10^7\ M^{-1}\ s^{-1}$ could be determined from the slopes of these plots. The result of the RK4 simulation successfully indicates that both reactions (6) and (7) occurred in the range of 1–150 μs in this system. The rate constants estimated here for the reactions (6) and (7) are much larger than those measured in other systems. The $k_{6s}$ value ($4.5 \times 10^5\ M^{-1}\ s^{-1}$) obtained with the stopped-flow measurements is more than one-order smaller than the $k_6$ value ($8.7 \times 10^6\ M^{-1}\ s^{-1}$) estimated from the Toc• decays in the range of 1–150 μs. Furthermore, the rate constant for the reaction between $O_2^{-\bullet}$ and ascorbate was reported to be $3.3 \times 10^5\ M^{-1}\ s^{-1}$ in $H_2O$ at pH 7.8 [21], which is nearly two-order smaller than the $k_7$ value ($6.9 \times 10^7\ M^{-1}\ s^{-1}$) estimated in the present study.

The reason for the discrepancies in $k_6$ and $k_7$ between the present results and the previous corresponding ones might be explained in the following way. In the stopped-flow measurements, the reaction between Toc• and VC would occur when Toc• diffuses in the bulk phase and reaches the reversed micelle containing VC, since Toc• and VC are dissolved in the separate solutions before mixing. On the other hand, in the laser photolysis measurements, VC in the water droplets of the reversed micelle can react not only with Toc• which reaches the reversed micelle after diffusion but also with Toc• located near the reversed micelle from the beginning. α-TocH has a lipophilic alkyl chain and a chromanol head group having some polarity. Thus, in aqueous micelle or biomembrane systems, α-TocH is known to be located not so far from the w/o interface region [46,47]. Also, in the AOT reversed micelle system, some fraction of α-TocH would be located near the w/o interface region around the micelles. In such situations, Toc• would be generated from α-TocH located near the w/o interface region. The broadened EPR spectrum of Toc• in the AOT solution (Fig. 4a) also suggests such surroundings around Toc•. The reaction between VC inside the reversed micelle and Toc• located near the micelle from the beginning should be much faster than the reactions which need the diffusion process in the bulk phase. In contrast, the remaining fraction of Toc• in the bulk phase should react with VC through the diffusion process in the later time region, as observed with the stopped-flow method.

The fast $O_2^{-\bullet}$ quenching by VC might be explained in a similar way. Some fraction of $O_2^{-\bullet}$ would be generated near or inside the reversed micelle because the $O_2^{-\bullet}$ precursor ($e^-_{solv}$) was generated together with Toc•. Furthermore, $O_2^{-\bullet}$ would tend to dissolve in the water inside the reversed micelle since $O_2^{-\bullet}$ is hydrophilic. There, a fast quenching reaction of $O_2^{-\bullet}$ by VC would be expected. The local VC concentration in water droplets inside the micelle should be 100 times as large as the total concentration in the solution (w/o = 1/100). Thus, the apparent rate constant in the reversed micelle system ($k_7$) could be more than 100 times of that in aqueous solutions.

Another explanation might be possible for the large $k_7$ value. The water droplets inside the AOT reversed micelle should be acidic because of dissolved VC. For example, pH value of a VC aqueous solution ([VC] = 0.01 M) was 3.11. On the other hand, the AOT head group (sodium sulfosuccinate) should be concentrated in the water droplets inside the AOT reversed micelle. This situation should affect on pH in the water droplets. The pH value measured for an aqueous solution containing VC (0.01 M) and AOT (0.025 M) was 3.37. In the water droplets inside the micelle, pH value might be larger than 3.37 due to the concentrated AOT head group. Around pH = 3.4, most of VC should exist as the non-dissociated form. On the other hand, under acidic condition, $O_2^{-\bullet}$ would change to •OOH. •OOH can react to Toc• as well as $O_2^{-\bullet}$, and the rate constant for the reaction between Toc• and •OOH is thought to be very large. If $O_2^{-\bullet}$ enters into the acidic water droplets, •OOH would be generated, and would react with VC. As a result, it would be possible that •OOH participates in the Toc• decay kinetics. In our method, there is no way to separate the reactions of Toc• to $O_2^{-\bullet}$ and •OOH. However, the simultaneous rate equations (Eqs. (10) and (11)) can be used for •OOH as replacing [$O_2^{-\bullet}$] by [•OOH]. In this way, the analyses of the transient absorption data can be done successful. Then, the large $k_7$ value might be explained from higher reactivity of •OOH than that of $O_2^{-\bullet}$. However, we wonder the rate constant for the reaction between •OOH and VC would be more than 100 times of that for $O_2^{-\bullet}$. Moreover, the large rate constant ($k_6$) for the reaction between Toc• and VC cannot be explained in this way. In the AOT reversed micelle system, the surfactant AOT should mainly be controlled the property in the o/w interface region. We think some fraction of Toc• was trapped around the sulfosuccinate moieties of AOT placed in the middle area between the bulk oil phase and the water droplet, and it could rapidly react to VC in the water droplet.

In the present laser photolysis study, we found the fast quenching reactions of Toc• and $O_2^{-\bullet}$ by VC occurring around the reversed micelle and analyzed them with the RK4 simulation. The results show that fast kinetics of $O_2^{-\bullet}$ located near the reversed micelle can be investigated by observing Toc• as a probe. In this system, some fractions of Toc• and $O_2^{-\bullet}$ might be trapped around the reversed micelle, so that the fast quenching of Toc• and $O_2^{-\bullet}$ by VC occurred.

## 4. Conclusion

The $O_2^{-\bullet}$ quenching kinetics in w/o interface region of AOT reversed micelle has been investigated with the transient absorption method. Photodecomposition of TocH in the solution containing $O_2$ produced $O_2^{-\bullet}$ together with Toc•. The subsequent reaction occurred between Toc• and $O_2^{-\bullet}$ in the time region of 1–150 μs after the photoexcitation. There, $O_2^{-\bullet}$ decay dynamics could be traced by monitoring Toc•. In an AOT reversed micelle solution containing VC, VC would be located in water droplets inside the reversed micelle and would react with both Toc• and $O_2^{-\bullet}$ in the w/o interface region around the reversed micelle. The Toc• decay in the time region of 1–150 μs was accelerated by addition of VC, suggesting that the $O_2^{-\bullet}$ quenching by VC progressed as well as the Toc• quenching by VC. From the numerical RK4 simulation with treating the simultaneous rate equations for Toc•, the rate constants for $O_2^{-\bullet}$ quenching and Toc• quenching by VC could be estimated to be $6.9 \times 10^7\ M^{-1}\ s^{-1}$ and $8.7 \times 10^6\ M^{-1}\ s^{-1}$, respectively. These values are much larger than the corresponding values reported in homogeneous solutions, suggesting that these quenching reactions occurred indeed at the w/o interface of the reversed micelle.

## Acknowledgement

This work was supported by Grant-in-Aid for Scientific Research C (Nos. 19550019 and 22590038) from the Japan Society for the Promotion of Science (JSPS).

## References

[1] E. Niki, Free Radic. Res. 33 (2000) 693–704.
[2] R.G. Cutler, Free Radic. Biol. 6 (1984) 371–428.
[3] B. Halliwell, J.M.C. Gutteridge, C.E. Cross, J. Lab. Clin. Med. 119 (1992) 598–620.
[4] L.R.C. Barclay, Can. J. Chem. 71 (1993) 1–16.
[5] E. Niki, Chem. Phys. Lipids 44 (1987) 227–253.
[6] G.W. Burton, T. Doba, E.J. Gabe, L. Hughes, F.L. Lee, L. Prasad, K.U. Ingold, J. Am. Chem. Soc. 107 (1985) 7053–7065.

[7] G.W. Burton, K.U. Ingold, Acc. Chem. Res. 19 (1986) 194–201.
[8] B. Halliwell, Annu. Rev. Nutr. 16 (1996) 33–50.
[9] I.S. Young, J.V. Woodside, J. Clin. Pathol. 54 (2001) 176–186.
[10] M.R. Olthof, P.C.H. Hollman, M.B. Katan, J. Nutr. 131 (2001) 66–71.
[11] J.-K. Moon, T. Shibamoto, J. Agric. Food Chem. 57 (2009) 1655–1666.
[12] G. Cao, H.M. Alessio, R.G. Cutler, Free Radic. Biol. Med. 14 (1993) 303–311.
[13] D. Huang, B. Ou, R.L. Prior, J. Agric. Food Chem. 53 (2005) 1841–1856.
[14] P. Stocker, J.-F. Lesgards, N. Vidal, F. Chalier, M. Prost, Biochim. Biophys. Acta 1621 (2003) 1–8.
[15] B. Ou, M. Hampsch-Woodill, R.L. Prior, J. Agric. Food Chem. 49 (2001) 4619–4626.
[16] I. Fridovich, Science 201 (1978) 875–880.
[17] E. Welles Kellogg III, I. Fridovich, J. Biol. Chem. 250 (1975) 8812–8817.
[18] Y. Mao, L. Zang, X. Shi, Biochem. Mol. Biol. Int. 36 (1995) 227–232.
[19] I. Fridovich, Annu. Rev. Pharmacol. Toxicol. 23 (1983) 239–257.
[20] D. Taubert, T. Breitenbach, A. Lazar, P. Censarek, S. Harlfinger, R. Berkels, W. Klaus, R. Roesen, Free Radic. Biol. Med. 35 (2003) 1599–1607.
[21] N. Gotoh, E. Niki, Biochim. Biophys. Acta 1115 (1992) 201–207.
[22] C.C. Trevithick-Sutton, C.S. Foote, M. Collins, J.R. Trevithick, Mol. Vis. 12 (2006) 1127–1135.
[23] J.F. Ewing, D.R. Janero, Anal. Biochem. 232 (1995) 243–248.
[24] K.L. Quick, J.I. Hardt, L.L. Dugan, J. Neurosci. Methods 97 (2000) 139–144.
[25] H. Zhao, S. Kalivendi, H. Zhang, J. Joseph, K. Nithipatikom, J. Vásquez-Vivar, B. Kalyanaraman, Free Radic. Biol. Med. 34 (2003) 1359–1368.
[26] W.F. Beyer Jr., I. Fridovich, Anal. Biochem. 161 (1987) 559–566.
[27] K. Faulkner, I. Fridovich, Free Radic. Biol. Med. 15 (1993) 447–451.
[28] S.V. Jovanovic, Y. Hara, S. Steenken, M.G. Simic, J. Am. Chem. Soc. 117 (1995) 9881–9888.
[29] S.V. Jovanovic, S. Steenken, M. Tosic, B. Marjanovic, M.G. Simic, J. Am. Chem. Soc. 116 (1994) 4846–4851.
[30] K. Ohara, A. Shimizu, Y. Wada, S. Nagaoka, J. Photochem. Photobiol. A 210 (2010) 173–180.
[31] R.H. Bisby, A.W. Parker, FEBS Lett. 290 (1991) 205–208.
[32] R.H. Bisby, A.W. Parker, Arch. Biochem. Biophys. 317 (1995) 170–178.
[33] M.H. Carpenter, C.A. Kennedy, H. Bijl, S.A. Viken, V.N. Vatsa, J. Sci. Comput. 25 (2005) 157–194.
[34] J.C. Butcher, The Numerical Analysis of Ordinary Differential Equations, John Wiley, New York, 1987.
[35] K. Mukai, A. Ouchi, A. Mitarai, K. Ohara, C. Matsuoka, Bull. Chem. Soc. Jpn. 82 (2009) 494–503.
[36] K. Ohara, Y. Hashimoto, C. Hamada, S. Nagaoka, J. Photochem. Photobiol. A 200 (2008) 239–245.
[37] H. Yamada, Y. Yamashita, M. Kikuchi, H. Watanabe, T. Okujima, H. Uno, T. Ogawa, K. Ohara, N. Ono, Chem. Eur. J. 11 (2005) 6212–6220.
[38] K. Ohara, A. Fujii, Y. Ichimura, K. Sato, K. Mukai, Bull. Chem. Soc. Jpn. 79 (2006) 421–426.
[39] E.B. De Borba, C.L.C. Amaral, M.J. Politi, R. Villalobos, M.S. Baptista, Langmuir 16 (2000) 5900–5907.
[40] V. Calvo-Perez, G.S. Beddard, J.H. Fendler, J. Phys. Chem. 85 (1981) 2316–2319.
[41] A.J.W.G. Visser, J.H. Fendler, J. Phys. Chem. 86 (1982) 947–950.
[42] S.L. Murov, Handbook of Photochemistry, Macel Dekker, New York, 1973.
[43] S. Nagaoka, T. Kakiuchi, K. Ohara, K. Mukai, Chem. Phys. Lipids 146 (2007) 26–32.
[44] G.P. Laroff, R.W. Fessenden, R.H. Schuler, J. Am. Chem. Soc. 94 (1972) 9062–9073.
[45] K. Ohara, R. Watanabe, Y. Mizuta, S.I. Nagaoka, K. Mukai, J. Phys. Chem. B 107 (2003) 11527–11533.
[46] K. Fukuzawa, W. Ikebata, A. Shibata, I. Kumadaki, T. Sakanaka, S. Urano, Chem. Phys. Lipids 63 (1992) 69–75.
[47] K. Fukuzawa, W. Ikebata, K. Sohmi, J. Nutr. Sci. Vitaminol. (Tokyo) 39 (Suppl.) (1993) S9–S22.